frontiers | Frontiers in Marine Science

TYPE Original Research
PUBLISHED 04 August 2022
DOI 10.3389/fmars.2022.948772

OPEN ACCESS

EDITED BY
Marta Plavsic,
Rudjer Boskovic Institute, Croatia

REVIEWED BY
Claire P. Till,
Cal Poly Humboldt, United States
Sotirios Karavoltsos,
National and Kapodistrian University of Athens, Greece
Randelle M. Bundy,
University of Washington, United States

*CORRESPONDENCE
Abigail J.R. Smith
Abigail.Smith@utas.edu.au

SPECIALTY SECTION
This article was submitted to Marine Biogeochemistry, a section of the journal Frontiers in Marine Science

RECEIVED 20 May 2022
ACCEPTED 12 July 2022
PUBLISHED 04 August 2022

CITATION
Smith AJR, Nelson T, Ratnarajah L, Genovese C, Westwood K, Holmes TM, Corkill M, Townsend AT, Bell E, Wuttig K and Lannuzel D (2022) Identifying potential sources of iron-binding ligands in coastal Antarctic environments and the wider Southern Ocean. *Front. Mar. Sci.* 9:948772. doi: 10.3389/fmars.2022.948772

Identifying potential sources of iron-binding ligands in coastal Antarctic environments and the wider Southern Ocean

Abigail J.R. Smith[1]*, Talitha Nelson[1], Lavenia Ratnarajah[2], Cristina Genovese[3], Karen Westwood[4,5], Thomas M. Holmes[5], Matthew Corkill[1], Ashley T. Townsend[6], Elanor Bell[4], Kathrin Wuttig[7] and Delphine Lannuzel[1]

[1]Institute for Marine and Antarctic Studies, University of Tasmania, Hobart, TAS, Australia, [2]Department of Earth, Ocean and Ecological Sciences, University of Liverpool, Liverpool, United Kingdom, [3]Department of Géosciences, Environnement et Societé, Université Libre de Bruxelles, Bruxelles, Belgium, [4]Australian Antarctic Division, Department of Agriculture, Water and the Environment, Kingston, TAS, Australia, [5]Australian Antarctic Program Partnership, University of Tasmania, Hobart, TAS, Australia, [6]Central Science Laboratory, University of Tasmania, Hobart, TAS, Australia, [7]Antarctic Climate and Ecosystems Cooperative Research Centre, Hobart, TAS, Australia

The availability of iron (Fe) to marine microbial communities is enhanced through complexation by ligands. In Fe limited environments, measuring the distribution and identifying the likely sources of ligands is therefore central to understanding the drivers of marine productivity. Antarctic coastal marine environments support highly productive ecosystems and are influenced by numerous sources of ligands, the magnitude of which varies both spatially and seasonally. Using competitive ligand exchange adsorptive cathodic stripping voltammetry (CLE-AdCSV) with 2-(2-thiazolylazo)-*p*-cresol (TAC) as a competing artificial ligand, this study investigates Fe-binding ligands (FeL) across the continental shelf break in the Mertz Glacier Region, East Antarctica (64 - 67°S; 138 - 154°E) during austral summer of 2019. The average FeL concentration was 0.86 ± 0.5 nM Eq Fe, with strong conditional stability constants (Log K_{FeL}) averaging 23.1 ± 1.0. The strongest binding ligands were observed in modified circumpolar deep water (CDW), thought to be linked to bacterial Fe remineralisation and potential siderophore release. High proportions of excess unbound ligands (L') were observed in surface waters, as a result of phytoplankton Fe uptake in the mixed layer and euphotic zone. However, FeL and L' concentrations were greater at depth, suggesting ligands were supplied with dissolved Fe from upwelled CDW and particle remineralisation in benthic nepheloid layers over the shelf. Recent sea-ice melt appeared to support bacterial production in areas where Fe and ligands were exhausted. This study is included within our newly compiled Southern Ocean Ligand (SOLt) Collection, a database of publicly available Fe-binding ligand surveys performed south of 50°S. A review of the SOLt Collection brings attention to the paucity of ligand data collected along the East Antarctic coast and the difficulties in pinpointing sources of Fe and ligands in coastal environments. Elucidating poorly understood ligand sources is essential to

predicting future Fe availability for microbial populations under rapid environmental change.

KEYWORDS

Fe availability, microbial productivity, benthic nepheloid layers, SOLt collection, complexation

1 Introduction

Sub-nanomolar concentrations of dissolved iron (dFe), together with light, are a well-acknowledged limitation on Southern Ocean primary productivity (Martin et al., 1990; Sedwick et al., 2000; Boyd et al., 2007). Loss mechanisms, including scavenging onto particles and rapid uptake by phytoplankton, result in low surface water concentrations of free Fe (Fe'), with estimates between 9 – 125 pM (Morel et al., 2008; Sarthou et al., 2011). Ligands are organic or inorganic molecules which chelate Fe to form a complex, preventing scavenging and increasing the residence time of Fe in surface waters (Gledhill and Buck, 2012; Boyd and Ellwood, 2010; Johnson et al., 1997; Tagliabue et al., 2019). Ligands complex more than 99% of dFe in seawater (Gledhill and Buck, 2012), and increase the bioavailability of Fe to phytoplankton and bacteria in limiting environments such as the Southern Ocean (Hassler et al., 2011).

Ligands comprise a vast range of molecules from many different sources. Inorganic ligands may bind Fe as oxides or oxyhydroxides and may be released with mineral Fe from hydrothermal vents (Waite and Morel, 1984; Cunningham et al., 1988; Wu et al., 2001; Toner et al., 2009). Organic ligands produced by biological processes include extracellular polymeric substances (EPS) exuded by phytoplankton (Hassler et al., 2011; Shaked and Lis, 2012; Hassler et al., 2017) and humic or humic-like substances (HS or HS-like) typically from estuaries, rivers, or biological degradation products (Laglera and van den Berg, 2009; Whitby et al., 2020). Some of the strongest ligands are actively produced by bacteria under Fe stress, known as siderophores (Gledhill et al., 2004; Boiteau et al., 2016; Bundy et al., 2016).

Both abiotic and biotic processes contribute ligands to coastal marine environments. Elevated organic ligand concentrations are commonly associated with surface water deep chlorophyll maxima (DCM), where a combination of algae exudates and bacterial siderophores contribute ligands in excess of Fe concentrations (Boye et al., 2001; Hogle et al., 2018). Additionally, high concentrations of ligands have been observed in sea ice (up to 34.4 nM Eq Fe of uncomplexed ligands, L'), thought to originate from organic material incorporated during ice growth (Janssens et al., 2018) and microbial ligand production within brine channels (Bowman, 2013). These ligands may be released into seawater with sea-ice melt, increasing the degree of Fe complexation in spring and summer (Lannuzel et al., 2015; Genovese et al., 2018). Sediment resuspension and benthic nepheloid layers have also been observed to contribute ligands near the seafloor (Bundy et al., 2014).

Despite an increase in spatial coverage of Fe and ligand data from the Southern Ocean (Thuróczy et al., 2011; Thuróczy et al., 2012; Caprara et al., 2016; Gerringa et al., 2020; Hassler et al., 2020a; Ardiningsih et al., 2021a and references therein) studies seldom focus on coastal environments which are particularly sensitive to climate-induced changes. The Mertz Glacier Region (64 - 67°S; 138 - 154°E, off George V and Adélie Land, East Antarctica), is a globally important and valuable coastal region for global thermohaline circulation and ecological productivity. Intense phytoplankton blooms within the Mertz polynya make the region a biological hotspot (McMahon et al., 2002; Sambrotto et al., 2003; Ropert-Coudert et al., 2018) and the production of Dense Shelf Waters via sea-ice formation contributes to a quarter of total Antarctic Bottom Water production (Bindoff et al., 2000, Williams et al., 2008; Williams et al., 2010; Cougnon et al., 2013). With the calving of the Mertz Glacier Tongue in 2010, this region has already experienced dramatic changes in processes which influence productivity (Tamura et al., 2012; Liniger et al., 2020; Shadwick et al., 2013). Yet the mechanisms underpinning this productivity (such as Fe supply and availability through complexation with ligands) remain elusive.

In this study, we examine potential sources controlling the Fe-binding ligand distribution in the highly productive Mertz Glacier Region. We compare the speciation of Fe between the surface and deeper waters and consider the influence of the continental shelf and sea-ice melt, before comparing our data to the broader Southern Ocean using our newly compiled Southern Ocean Ligand (SOLt) collection. This dataset includes 25 iron-complexation studies performed in the Southern Ocean since 1995 and is accessible for future biogeochemical assessments. Using our new data and the SOLt collection, we aim to determine the processes associated with increased Fe-binding ligand concentrations, and to highlight existing gaps in our knowledge of Fe complexation across the Southern Ocean.

2 Methods

2.1 Study area

The ENRICH (Euphausiids and Nutrient Recycling in Cetacean Hotspots) voyage, onboard the RV *Investigator*, targeted waters off the coast of George V Land and Adélie Land, East Antarctica (64 - 67°S; 138 - 154°E, Figure 1). Seawater samples for ligand analysis were collected from 11 stations (20 – 1,200 m depth, approximately 9 samples per station depending on hydrographic features identified from CTD casts), between the 25th of January - 26th of February 2019. The region is characterised by a narrow continental shelf of approximately 400 m depth but deepens to 600 m in basins such as the Mertz and Adélie Depressions (Harris and Beaman, 2003).

The latent heat polynya in this region leads to intense chlorophyll blooms in front of the Mertz Glacier during the summer months (Figure 1). In the months leading up to the survey, satellite data showed the December 2018 sea-ice extent (SIE, classified as ≥15% sea-ice concentration) reached 65°S, covering the location of Stations 10, 14 and 16 on the shelf. By February 2019 (during our sampling), sea ice had retreated further inshore. To assess sources and cycling processes of Fe-binding ligands across the region, stations were divided into three groups based on their proximity to the continental shelf, comprising Shelf (10, 14, 16 and 17), Slope (11 and 18) and Offshore (1, 9, 12, 15 and 19) stations.

2.2 Hydrography and bacterial production

Hydrographic parameters including salinity, temperature, depth, oxygen, light transmittance, chlorophyll-*a* (Chl-*a*) fluorescence, and photosynthetically active radiation (PAR) were measured at each station from CTD casts down to 1,200 m. Water masses were determined using neutral density definitions from the nearby Ross Sea (Orsi and Wiederwohl, 2009). Fronts were identified from sub-surface temperature isotherms with the Southern Antarctic Circumpolar Front (SACCF) at the 1.8°C isotherm and the Antarctic Slope Front (ASF) at 0°C (Orsi et al., 1995; Williams et al., 2010), using both ENRICH CTD profiles and Argo profiles (Australian Ocean Data Network, AODN) between December 2018 – February 2019. Mixed layer depths (MLD) were defined using a potential density threshold of $\Delta\sigma_\theta$ = 0.03 kg m^{-3} (de Boyer Montégut et al., 2004) and euphotic depths (Z_{eu}) were defined as 1% of surface photosynthetically active radiation (PAR, Vaillancourt et al., 2003; Lehmann et al., 2004).

Benthic nepheloid layers were identified using a Wetlabs C-STAR Transmissometer (25 cm pathlength with 650 nm wavelength, calibrated in air and clean water) for shelf stations only. Beam Attenuation Coefficient (c, m^{-1}) was calculated by,

$$c = -\left(\frac{1}{r}\right) * \ln\left(\frac{Tr}{100}\right)$$

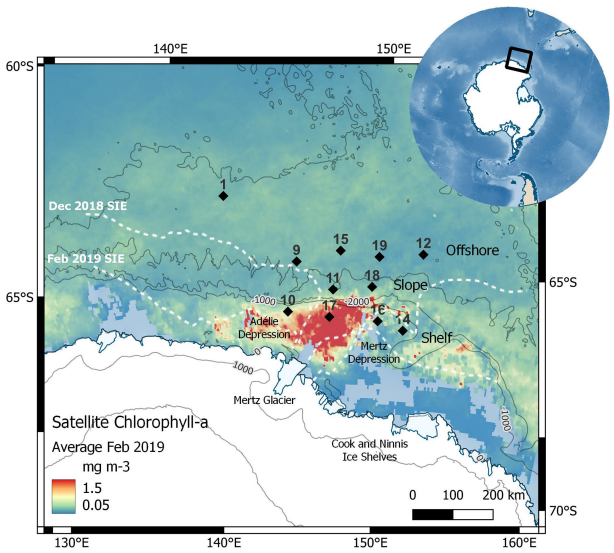

FIGURE 1
Survey sampling stations (black diamonds) within the Mertz Glacier Region. Background colour shows monthly average satellite chlorophyll-*a* (Chl-*a*) concentration for February (NASA Giovanni MODIS-Aqua). Monthly average sea-ice extent (SIE, ≥15% sea-ice concentration) for December 2018 and February 2019 (white dashed lines, Meier et al., 2021) and bathymetric contours (light grey solid lines, IBSCO) are shown. Stations were divided into three groups (Offshore, Slope, and Shelf) based on their proximity to continental shelf. Figure developed using the Norwegian Polar Institute's Quantarctica package (Matsuoka et al., 2018).

where, r is the beam path length of the transmissometer (0.25 m), and Tr is the transmission data (%). The particulate coefficient (cp) was calculated by subtracting the coefficient of clear seawater (csw); here defined as c from offshore Station 1, 1,200 m depth. The nepheloid boundary was then defined as the depth at which $cp = cp_{min} + 0.01$ (Gardner et al., 2018).

As in Westwood et al., (2018), bacterial production (BP) was determined using the Kirchman (2000) ^{14}C-leucine microcentrifuge method, with calculations using parameters specified by Smith and Azam (1992). Three replicates (and two controls) were taken for measurements of surface waters (10 m) and at the DCM at each station. Bacterial production and oceanographic parameters were used to determine co-variance between complexation parameters and environmental variables (using Pearson product-moment correlation coefficients, unless stated otherwise).

2.3 Seawater sampling

New 250mL Nalgene© LDPE (low density polyethylene) sample collection bottles were cleaned in 2% (v:v) Decon-90 detergent for one week, rinsed four times with deionised water and thrice in ultra-high purity (UHP) water. The bottles were filled with 6M hydrochloric acid (HCl) and placed in a 1.2M HCl bath for one month. Following acid cleaning, bottles were rinsed with UHP to remove remaining acid, at least four times. Bottles were rinsed thrice with freshly collected filtered (<0.2 µm) seawater prior to sampling.

A Trace Metal Rosette (TMR; General Oceanics Inc., Miami, FL, USA) with 12x 10L Teflon-lined Niskin bottles was used to sample trace elements and ligands from the water column. Seawater from each depth was sampled within a trace-metal-clean laboratory onboard, beneath ISO 5 HEPA filtered air and using acid-cleaned and seawater flushed AcroPak™ 0.2 µm filter cartridges, following GEOTRACES protocols (Cutter et al., 2017). Samples were stored frozen at -20°C until voltammetric analysis onshore.

2.4 Dissolved iron

Analysis of dFe was previously described in Smith et al. (2021), following methods developed in Wuttig et al. (2019). Briefly, dissolved trace elements were preconcentrated from seawater using an offline seaFAST preconcentration system (SC-4 DX seaFAST S2/*pico*, ESI, Omaha, NE, USA) and concentrations were determined using a Thermo Fisher Scientific ELEMENT 2 SF-ICP-MS (Central Science Laboratory, University of Tasmania; medium resolution mode, Wuttig et al., 2019). Detailed methodology, certified reference material analyses, blanks, and detection limits for the ENRICH dFe dataset are given in Smith et al. (2021).

2.5 Iron-binding ligands

Competitive Ligand Exchange Adsorptive Cathodic Stripping Voltammetry (CLE-AdCSV) was used to determine Fe complexation parameters using TAC (2-(2-thiazolylazo)-*p*-cresol; Croot and Johannsson, 2000) as an artificial ligand. Seawater samples (125 mL) were defrosted at room temperature, buffered with 1 M boric acid buffer (1 M H_3BO_3/ 0.25 M NH_4^+OH, Sigma-Aldrich, St Louis, MO, USA/SeaStar Baseline, Sidney, BC, Canada) to a final concentration of 5 mM, and pH 8.05. Twelve preconditioned 10 mL polypropylene vials were spiked with increasing Fe concentrations (0 - 8 nM). Ten mL of buffered sample was added to each vial and a preconditioned Teflon cell and left to equilibrate for 1 h. The artificial ligand TAC (Sigma-Aldrich) was then added to each aliquot at a final concentration of 10 µM. Samples were left to equilibrate at room temperature overnight (> 5 h), with analysis the following day.

2.5.1 Voltammetric methods and calculations

Samples were analyzed using a Metrohm (Herisau, Switzerland) 797 VA voltameter equipped with a hanging mercury drop electrode (HMDE), a glassy carbon auxiliary electrode, and a Ag/AgCl reference electrode with a 3 M KCl salt bridge. Each aliquot was purged with ultrapure N_2 gas for 240 s prior to analysis. Using differential pulse mode, an adsorption potential of -0.4 V was applied for 480 – 600 s (depending on natural dFe concentration of sample) and scanned from -0.4 – -0.9 V. Voltage steps occurred over 2.55 mV at 0.1 s, and modulation from 49.95 mV over 0.01 s. Duplicate measurements of peak height (I, nA) and potential (V) were recorded for the titration curve and slope. Blank measurements were performed on UV-treated, bulk surface water (dFe < 0.03 nM) collected at Station 18 using standard addition methods (Fe^{3+} solution from 0 – 5 nM). Titration data was analysed using the complete complexation fitting model of ProMCC software (Omanović et al., 2015). Artificial ligand (AL) specifications for $Fe(TAC)_2$ included a conditional stability constant (Log $K_{Fe(TAC)2}$) = 22.4 and an inorganic side reaction coefficient (α) = 1, giving $\alpha(Fe(TAC)_2)$ = 251 for 10 µM TAC. From these calculations, total ligand concentration (Lt = FeL + L'), Fe-bound ligand concentration (FeL), free ligand concentration (L' = Lt - dFe), free Fe concentration (Fe' = free Fe + inorganically bound Fe), the ratio between total ligands and dissolved Fe (Lt:dFe, conditional stability constants for Fe-bound ligands (Log K_{FeL}) and side reaction coefficients (Log α = log(K_{FeL} × Lt)) could be determined.

2.5.2 2-(2-Thiazolylazo)-*p*-cresol correction

Iron contamination was found in titration blanks and confirmed using ICP-MS to be from the TAC reagent (Sigma-Aldrich). Standard addition experiments revealed our TAC

solution added an additional 1.98 ± 0.2 nM dFe (n = 6) to each aliquot. To account for reagent contamination, blank measurements were subtracted from our calculations. The limit of detection (LOD, taken as 3σ of the blank) was 0.36 nM Eq Fe. As a consequence of this contamination, a single ligand group was measured which represents an average of all ligand groups present.

TAC contaminations (up to 0.5 nM Fe) have been reported previously, resulting in high standard deviations for K' (Gerringa et al., 2015; Buck et al., 2016). Presently, no suitable method has been determined to clean Fe from artificial ligands and the extent of contamination appears to vary between batches and distributors.

2.6 Southern Ocean Ligand (SOLt) Collection

To compare data collected from the Mertz Region with other Southern Ocean studies, we compiled publicly available Fe complexation datasets from >50°S, to form the SOLt Collection. Studies which provided spatial reference coordinates, sampling dates, sampling depth, dFe, Lt and Log K_{FeL} were included. Control stations from incubation experiments performed in the Southern Ocean were also included (experimental treatments were excluded). Ligand concentrations were included as Lt or L1 (due to variability in analytical methods, other weaker ligand classes if provided were excluded from this dataset). Consequently, values represent the pooled average or dominant ligand group present in a sample. Datasets typically provided either Log K_{FeL} or Log K'. Therefore, to maintain consistency when comparing data, Log K' was normalized by a factor of 10^{10} (Caprara et al., 2016). Some studies did not provide specific start and end dates for sampling periods, in which case dates were taken as the first and last dates of the month/s described (i.e., a study describes sampling period as 'January-February 2007' but does not list specific dates, therefore SOLt dates are listed as Start: 01/01/2007 and End: 28/02/2007).

The collection may be used for comparisons with future complexation studies in the Southern Ocean or for use in biogeochemical models (noting some discrepancies from analytical variability, see Section 3.5). The SOLt Collection, including data from this study, can be downloaded from the IMAS Metadata Catalogue (https://metadata.imas.utas.edu.au/).

3 Results and discussion

Iron-binding ligands are receiving increased scientific attention in relation to Fe bioavailability to microbial communities. However, there are many processes that may influence Fe and ligand cycles across coastal regions, and these can vary both spatially and temporally. In spring, deep winter mixing coupled with diapycnal diffusion allow the supply of Fe into surface waters of the broader Southern Ocean (Tagliabue et al., 2014) but, closer to the continent shelf sediments and sea ice represent the dominant sources of Fe (Graham et al., 2015; Lannuzel et al., 2016). In the open ocean, supply of Fe from deep winter mixing only lasts a few days to weeks (Boyd et al., 2012), whereas closer to the continent sea-ice melt continues into February (Eayrs et al., 2019). Moving into summer and autumn (i.e., following sea-ice melt and supply for the subsurface reservoir), biological recycling represents the key mechanism for Fe supply in both the open ocean and coastal Antarctic waters (Tagliabue et al., 2019). Iron and ligand supply are tightly coupled; therefore, ligand sources likely differ both spatially and temporally. This study was undertaken in a coastal region in late summer where biological recycling dominated. Below we identify and discuss the main drivers of ligand concentrations in surface and deep waters within this region and the wider Southern Ocean.

3.1 Complexation of Fe in waters across the Mertz Region

In this survey of the Mertz Region, trace element and speciation samples were measured from five key water masses including Antarctic Surface Water (AASW), Upper and Lower Circumpolar Deep Waters (UCDW and LCDW), modified Circumpolar Deep Water (mCDW) and Dense Shelf Water (DSW, Figure 2). In AASW, mixed layers ranged from 22 – 54 m deep, and euphotic depths reached 32 – 77 m. Upper and LCDW were present offshore (Figure 2) and drove the southern extension of the SACCF inshore. Intrusions of LCDW onto the shelf were observed at Station 16. Over the shelf, DSW mixed with LCDW to form oxygenated mCDW. No Ice Shelf Water (ISW) was detected at any station. At the slope, DSW and mCDW extending from the shelf break were carried west by the Antarctic Slope Current (ASC, Williams et al., 2010). The full distribution of major oceanographic fronts and water masses during the study period are described by Smith et al. (2021).

Across the survey area, mean Lt concentration was 0.87 ± 0.5 nM Eq Fe, mean Log K_{FeL} = 23.2 ± 1.0 and Log α = 14.6 ± 0.9. Concentrations of Lt, L' and dFe were consistently greater at depth (> 100 m), compared to surface waters (t = -2.2, P = 0.007, df = 40, Student's t-test, Figure 3). Ligands were always in excess of Fe concentrations, with the largest discrepancies noted at the surface where Lt:dFe ratios ranged from 22.9 - 39.6 (Figure 2F).

On the shelf, Lt concentrations associated with DSW were double the concentrations observed in AASW (Figure 2A, D). Shelf mCDW was found to have the strongest mean complexing capacity (LogK_{FeL} = 24.6 ± 1.9, Station 10, 280m, Figure 3) with moderate Lt concentrations (1.09 ± 0.6 nM Eq Fe). Slope waters exhibited the overall greatest mean concentration of Lt associated with LCDW (1.16 ± 0.58 nM Eq Fe, Figure 2D).

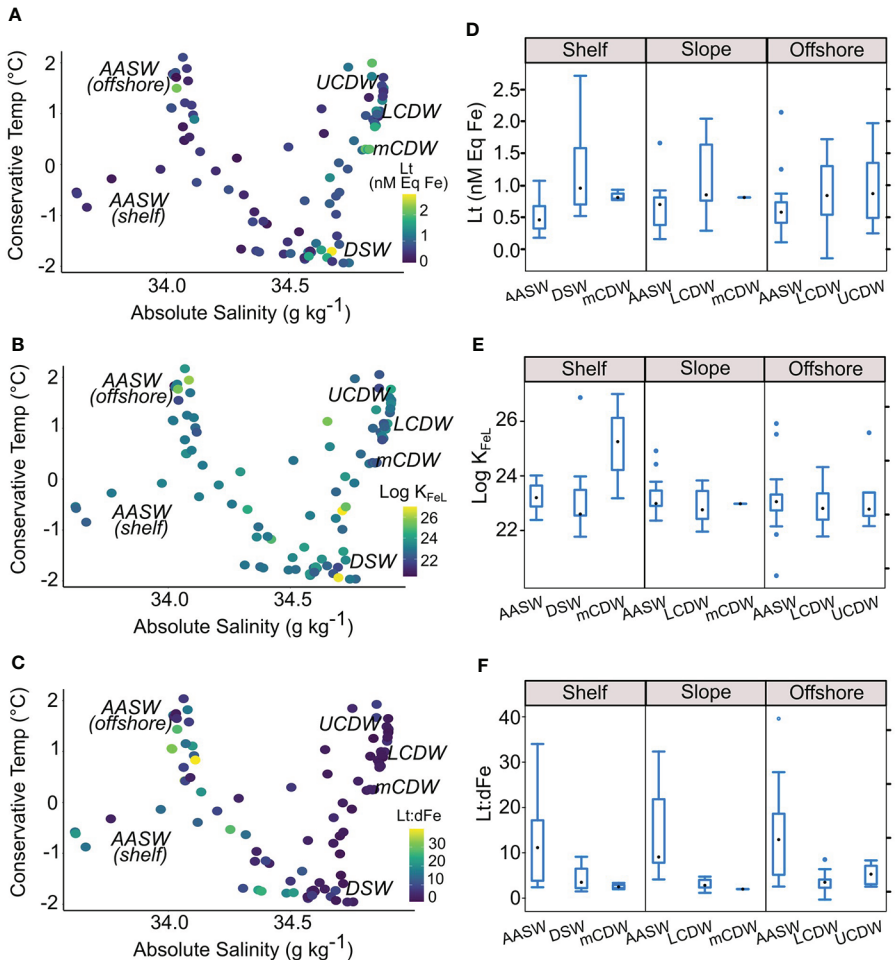

FIGURE 2
Temperature–salinity diagram representing Lt **(A)**, Log K_{FeL} **(B)** and Lt:dFe **(C)** in water masses present across the region. Box-and-Whisker plot illustrating Lt **(D)**, Log K_{FeL} **(E)** and the Lt:dFe ratios **(F)** across water masses and frontal regions (including shelf, slope and offshore). AASW: Antarctic Surface Water, UCDW: Upper Circumpolar Deep Water, LCDW: Lower Circumpolar Deep Water, mCDW: modified Circumpolar Deep Water, DSW: Dense Shelf Waters.

Compared to shelf and slope waters, Lt in offshore waters held the weakest mean complexing capacities ($LogK_{FeL}$ = 20.3, Station 12, 20 m). On average, offshore deep waters held the greatest concentration of Fe' and L' compared to shelf and slope stations (Figure 3).

3.2 Sea-ice melt

During December 2018, satellite data revealed that sea-ice area increased over the south-eastern sector of the study area and by February 2019 this ice cover was reduced (Supplementary Figure 1). Shelf stations 14 and 16 were covered by ice 19 days prior to sampling and were 50 – 70 km away from the sea-ice edge during the survey. Evidence of sea-ice melt was detected at Stations 14 and 16 by cool (θ = -1.12°C) and relatively fresh (S_A = 34.1 g kg^{-1}) surface waters (Figure 4). Absolute salinity (20 m) at Stations 14, 16 and 17 was 0.78 g kg^{-1} lower than offshore stations.

Fresh and cold surface waters measured at Stations 14 and 16 were most likely associated with the southward contraction of the sea-ice edge throughout February and corresponded with low surface concentrations of FeL and L', and marginally higher Fe' concentrations. At 20 m, Stations 14 and 16 showed mean surface Lt concentrations of 0.39 ± 0.1 and 0.62 ± 0.2 nM Eq Fe, respectively. Conditional stability constants did not vary with ice melt stations and Lt:dFe ratios remained intermediate. Unbound Fe (Fe') concentrations were greatest (1.90 pM) in surface waters of Station 16 where ice melt was evident, this trend extended west to Station 17 which was associated with low concentrations of L' (0.18 nM Eq Fe, Figure 4). No significant relationship was detected between surface Lt concentration and absolute salinity

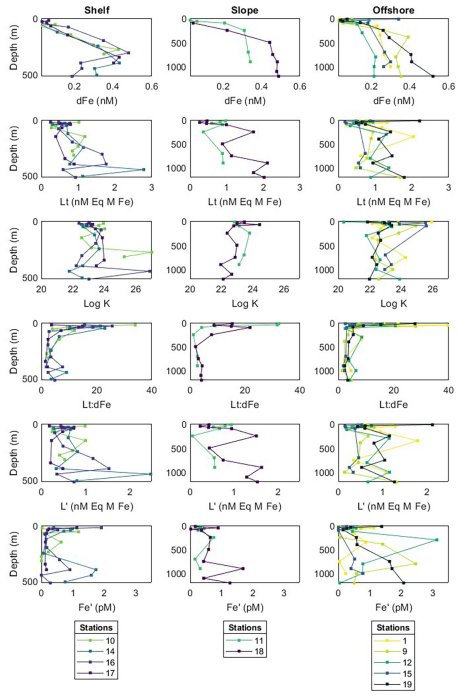

FIGURE 3
Depth profiles for dissolved Fe (dFe) and complexation parameters: total ligands (Lt), conditional stability constant (Log K_{FeL}), ratio of total ligands to dissolved Fe (Lt:dFe), ligands not bound to Fe (L') and Fe not bound to ligands (Fe'). Stations have been divided into offshore, slope and shelf groups, as shown in Figure 1.

(R = 0.02, P = 0.90), conservative temperature (R = 0.32, P = 0.16), nor latitude (R = 0.27, P = 0.22).

High concentrations of Lt have previously been observed in East Antarctic fast ice meltwater (up to 72 nM of Lt; Lannuzel et al., 2015) and pack ice meltwater (up to 41 nM of Lt; Genovese et al., 2018). The release of Fe and ligands from sea ice is dependent on seasonal melt and brine discharge. In early spring, brine inclusions in sea ice connect (due to enhanced sea-ice porosity) to form full-depth brine channels (Jardon et al., 2013) and are estimated to release up to 210 nmol m^2 d^{-1} of L' via gravity-driven brine convection (Hassler et al., 2017; Genovese et al., 2018). As the season progresses, diffusion takes over from convection (Tison et al., 2008) and is thought to slow the release of ligands into surface waters (Genovese et al., 2018) which may explain why complexation was low near sea-ice melt in the present study. This premise is further supported by studies in the Ross Sea, where both summer Lt and L' concentrations in ice-covered areas were reduced (compared to ice-free areas), suggesting the release of ligands from sea ice is highly variable or influenced by external uptake/supply mechanisms (Gerringa et al., 2020).

Polysaccharides, biopolymers, and HS-like aggregates produced by microbes (including sea-ice algae and bacteria) residing within sea-ice brine inclusions are thought to be a primary source of ligands (Calace et al., 2010; Lannuzel et al., 2015). However, rapid uptake of dFe by microbial communities makes identifying sources of Fe and associated Lt in surface waters difficult, particularly in late summer when recycling generally supports Fe supply (Boyd and Ellwood, 2010; Tagliabue et al., 2019).

3.3 Chlorophyll fluorescence and bacterial production

Satellite data products suggested that an intense phytoplankton bloom persisted during this study adjacent to the Mertz Glacier (Figure 1, Liniger et al., 2020). This bloom was confirmed by our *in-situ* results, where depth integrated Chl-*a* concentrations reached 68 mg m^{-2} at the DCM (58 m, Station 17). During the survey, however, greater Chl-*a* concentrations were measured offshore (Stations 1 and 15), reaching 148 mg m^{-2} (integrated to the DCM = 50 m).

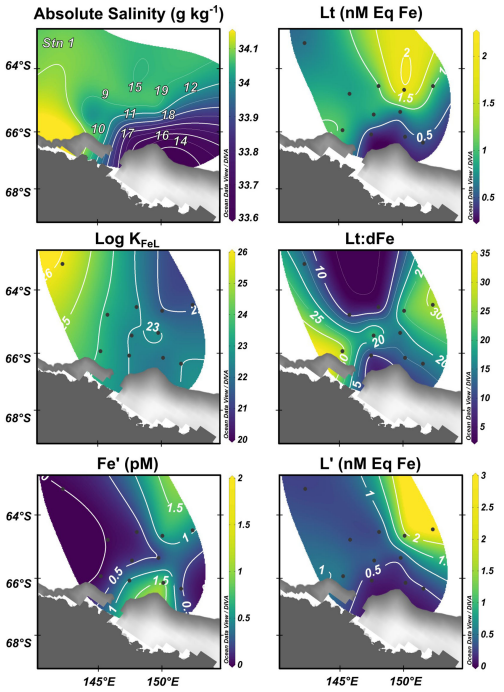

FIGURE 4
Surface (20 m) absolute salinity indicating recent sea ice melt, with Fe complexation parameters including total ligand concentration (Lt), conditional stability constant (Log K_{FeL}), total ligand to dissolved Fe ratio (Lt:dFe), free Fe (Fe') and free ligands (L') across survey area.

In surface waters, irradiance (PAR) showed a strong positive correlation with Lt, L' (both R = 0.6, P < 0.001) and Fe' (R = 0.4, P = 0.03). However, no significant relationship with fluorescence nor dissolved oxygen was observed, which may point to increased phytoplankton productivity (Supplementary Figure 2). Notably, Lt:dFe ratios were greatest within the euphotic zone (Figure 5) and correlated positively with fluorescence (R = 0.4, P < 0.001) and dissolved oxygen (R = 0.6, P < 0.001). At the center of the persistent Mertz bloom (Station 17), ligands were close to saturation at the surface (Lt:dFe = 3.68 at 20 m, Figure 4), but became less saturated near the DCM (Lt:dFe = 14.9 at 30 m). No relationship was observed between fluorescence and conditional stability constants nor Fe' in surface waters.

In surface waters, FeL exposed to UV irradiation can result in the dissociation of Fe from ligands. The photo-lability of FeL in surface waters increases Fe' which can be easily taken up by phytoplankton, and L' which can complex new additions of Fe (Croot and Heller, 2012; Hassler et al., 2020b). In addition, increased primary productivity in coastal regions can result in the biological production of L' (Thuróczy et al., 2012; Gerringa et al., 2020). In this study, L' were in excess with respect to dFe concentrations in the euphotic zone for all stations, and both Fe' and L' showed strong positive correlations with increasing irradiation (Supplementary Figure 2). Excess L' may be the result of photo-degradation and phytoplankton exudation. However, concentrations of FeL and L' increased with depth suggesting that Lt:dFe ratios were driven by Fe uptake by phytoplankton, rather than ligand production. As there was no significant relationship between ligands and Chl-*a* distribution in our study, it is likely that photo-degradation provided Fe' for phytoplankton uptake but cellular exudation made a small to negligible contribution to the excess ligand production during February.

Many studies highlight phytoplankton as primary ligand producers at the DCM, with metabolic processes producing a suite of ligands including exopolysaccharides (Boye et al., 2001; Hassler et al., 2017; Gerringa et al., 2020). In the late summer season, as phytoplankton blooms become senescent, increasing concentrations of exuded DOC (including EPS) are expected to contribute up to 80% of the surface ligand pool (Hassler et al., 2017). Studies showing that phytoplankton productivity is a source of ligands have commonly considered trends between complexation parameters and *in-situ* chlorophyll fluorescence (Croot et al., 2004; Thuróczy et al., 2012; Gerringa et al., 2020). However, co-occurring surface ligand sources and various sinks often mean the relationship between Lt and fluorescence is only weakly positive (albeit often significant due to large sample sizes typically collected). Ligands may be released during phytoplankton death through viral lysis (Poorvin et al., 2011; Slagter et al., 2016; Biggs et al., 2021) or 'sloppy feeding' by zooplankton (Rue and Bruland, 1997; Boye et al., 2001). In parallel, microbial endocytosis removes entire Fe-ligand complexes from the water column (Hutchins et al., 1999; Sutak et al., 2020). These natural fluxes hamper our interpretation of Lt supply mechanisms.

Bacterial production was highest at Station 14 (0.11 μg C L^{-1} h^{-1}) and Station 16 (0.16 μg C L^{-1} h^{-1}), compared to offshore stations where bacterial production was 2.3 times lower. As bacterial production was only measured in surface waters and at the DCM for this study, Apparent Oxygen Utilisation (AOU) was used to estimate microbial respiration in deeper waters.

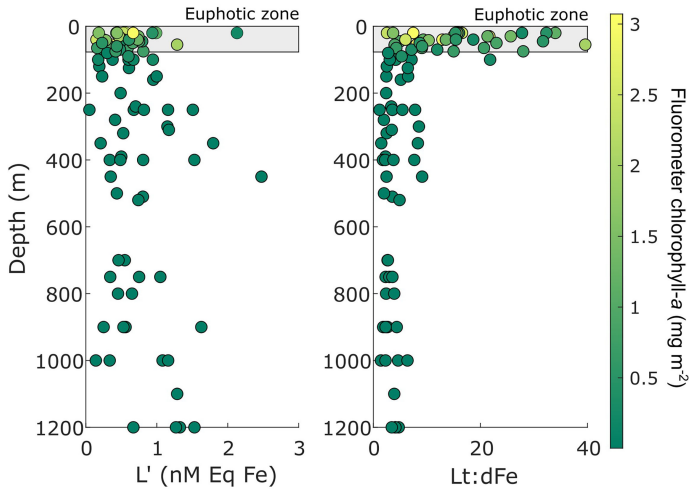

FIGURE 5
Free ligand (L') and total ligand-dissolved Fe ratio (Lt:dFe) profiles from the entire survey, coloured by chlorophyll fluorescence. Euphotic depth is represented by grey shaded box at a maximum depth of 55 m.

Positive correlations between dFe and AOU suggest bacteria remineralise Fe in AASW ($R = 0.54$, $P < 0.05$) and mCDW ($R = 0.64$, $P < 0.05$) along the slope (Smith et al., 2021). High levels of bacterial production at Stations 14 and 16, is also associated with sea-ice melt (Section 3.2). However, ligand parameters showed little relationship with bacterial production (Lt, $LogK_{FeL}$, Log α and L': $R = -0.24$, $P = 0.29$). A negative correlation between AOU (proxy of microbial respiration) and Lt:dFe was present ($R = -0.61$, $P < 0.001$). However, this is attributed to oxygen production and Fe uptake by phytoplankton in surface waters, leading to negative AOU values where excess ligands are found.

In comparison to the mean ENRICH survey Log K_{FeL} (23.2 ± 1.0), the relatively weak mean conditional stability constant (Log K_{FeL} = 22.7) of FeL present near sea-ice melt and bacterial production suggests that previous dFe release, or the moderate concentration of Fe' (1.9 pM) at the time of sampling, met bacterial Fe demands. Additions of Fe which release bacteria from Fe-limitation reduce the production of siderophores (Bundy et al., 2016), thereby reducing the overall $LogK_{FeL}$ of ligands in surrounding seawater. Strong negative correlations have also been observed between prokaryotic biomass and Lt concentration in the nearby Ross Sea, supporting the release of small concentrations of siderophores by bacteria (Rivaro et al., 2019). Bacterial degradation of organic ligands has been attributed to reduced Fe complexation in surface waters (Hassler et al., 2011). However, relationships between biomass (eukaryotic or prokaryotic) and Lt concentration are often unclear in environments with multiple nutrient sources and processes for organic matter degradation (Nolting et al., 1998; Boye et al., 2001; Rivaro et al., 2019; Gerringa et al., 2020).

3.4 Deeper waters

Over the whole study area, deeper waters (> 100 m) were 0.30 ± 0.04 nM higher in dFe, and 0.33 ± 0.03 nM Eq Fe higher in Lt compared to surface waters. Elevated Lt concentrations were most pronounced over the continental shelf, where DSW was found to double the concentration of Lt compared to shelf AASW (DSW mean Lt = 1.23 ± 0.67 nM Eq Fe). Additionally, ligands were closest to saturation in deep shelf waters (Lt:dFe = 3.09 ± 1.31). Across the ENRICH survey region, strong Fe-binding ligands (Log K_{FeL} > 22) were observed to complex Fe supplied from depth by upwelling CDW and resuspended sediments. The strongest complexing capacities were observed at the shelf break (~335 m, Log K_{FeL} = 26.9, Figure 3). At Station 14, vertical profiles of Fe' concentrations below 100m were consistent (mean 0.44 ± 0.5 pM), except for a peak of 1.73 pM at 400 m depth. Strong positive correlations with AOU, conservative temperature and absolute salinity suggested Fe' was supplied by LCDW (Supplementary Figure 2).

Nepheloid layers were recorded for shelf stations where suspended particles reduced seawater light transmittance near the seafloor, between 249 and 444 m depth and were on average 54 m thick. Stations 14 and 16 near the Mertz Depression had notably thicker nepheloid layers, reaching 222 m and 257 m above the seafloor, respectively (Supplementary Figure 3). Total ligand concentration integrated to 400 m (shallowest shelf station depth) was 52 – 95% greater at Stations 14 and 16 (0.82 and 1.00 nM Eq Fe m^{-1}, respectively) compared to Stations 10 and 17 (0.78 and 0.52 nM Eq Fe m^{-1}, respectively). In addition, L' concentrations peaked near the seafloor for Stations 14 and 16, reaching 1.5 – 2.4 nM Eq Fe at ~400 m. Microbial respiration (determined by AOU) positively correlated with $LogK_{FeL;}$ however, this relationship was not statistically significant ($R = 0.6$, $P = 0.27$, $n = 5$). In addition, the contribution of ice shelf basal melt to ligand supply could not be determined as ISW was not detected.

Iron remineralisation ratios were significant in both surface waters and mCDW, indicating microbial activity may be responsible for strong-ligand production in this region. It is probable that complexation by strong ligands enhances recycling of Fe during late summer, by preventing scavenging onto particles into the late season. While our Lt concentrations were in line with previous Southern Ocean studies, average Log K_{FeL} values were greater than other Antarctic coastal surveys (see Section 3.5, Table 1). For example, average Log K values of 22 were reported for shelf studies near the Pine Island and Thwaites glaciers (Thuróczy et al., 2012), as well as for the Ross Sea (Gerringa et al., 2020). Despite similar sampling seasons, Lt concentrations from our ENRICH study were approximately 3 times lower than those collected at the Mertz Glacier by Hassler et al. (2020a) in January 2017. Differences in complexation parameters between studies may be the result of analytical methods or regional and seasonal variability. For example, Hassler et al., sampled in very close range to the base of the Mertz Glacier (within 2 – 8 km based on the SCAR Antarctic Digital Database Coastline, medium resolution, updated January 2013), increasing the likelihood of sampling ligands from more coastal sources (i.e. ISW, sediments). In comparison, samples from the ENRICH voyage (Station 10) were 114 km farther from the base of the glacier.

In the ENRICH study, the highest concentrations of strong FeL were associated with intrusions of offshore CDW and shelf nepheloid layers. Lower CDW is a mixture of nutrient enriched NADW, Pacific, and Indian ocean waters (Carter et al., 2008), and has a circulation age of 295 years (Matsumoto, 2007). In the Atlantic, high Log K_{FeL} values have been attributed to North Atlantic Deep Waters (NADW) where strong ligands increase the residence time of Fe up to 1,039 years (Gerringa et al., 2015). Elevated strong ligand concentrations have also been recorded in LCDW in the Pacific (Buck et al., 2018); however microbial degradation and particle scavenging eventually deplete strong ligand concentrations in Pacific Deep Waters (PDW, up to 1,500 years old, England, 1995, Buck et al., 2018). Ligands in deep waters are typically

saturated with Fe due to particle remineralisation (Hassler et al., 2020b; Gerringa et al., 2015) and therefore are unlikely to act as a source of L' to surface waters. In addition, the FeL content of LCDW may be further enhanced by hydrothermalism and lateral advection within the Antarctic Circumpolar Current (Holmes et al., 2020; Janssen et al., 2020; Schine et al., 2021). Therefore, FeL entrained by LCDW which is upwelled onto the Mertz continental shelf may provide a possible explanation for the presence of strong binding ligands in this region.

On the shelf, FeL concentrations below the mixed layer are typically homogenous with depth (Buck et al., 2015), with the exception of regions influenced by features such as nepheloid layers which may elevate FeL concentrations above the benthos (Gerringa et al., 2020). In coastal regions, HS have been shown to be the dominant source of ligands in both surface waters and at depth, comprising up to 18% of the ligand pool (Bundy et al., 2014; Hassler et al., 2017). Humic substances are likely to be released by phytoplankton decomposition and resuspended detritus over the continental shelf (Calace et al., 2010; Hassler et al., 2017; Gerringa et al., 2020), however the detection of HS in seawater using CLE-CSV with TAC is sub-optimal (Laglera et al., 2011). Resuspended particles also increase the opportunity for bacterial remineralisation of refractory Fe and siderophore release (Velasquez et al., 2016; Homoky et al., 2021) and has been attributed to high concentrations of ligands reported near the continental shelf of Peru (Buck et al., 2018). This may have contributed to the strongest binding ligands observed in our study, however siderophores typically comprise a small percentage of the total ligand pool (Mawji et al., 2011).

Additionally, proximity to nearby ice shelves (Mertz Glacier and the Ninnis and Cook Ice Shelves) suggests glacial basal melt and ISW cannot be discounted as possible sources of FeL to shelf waters (Death et al., 2014; Dinniman et al., 2020). Ice Shelf Waters are formed *via* the inflow of relatively warm DSW into the Mertz Glacier cavity (Silvano et al., 2016); however, no ISW was directly detected in this study, likely due to sampling distance from the glacier base and mixing between shelf and offshore waters. Furthermore, the role of inorganic colloids (such as Fe oxyhydroxides) in binding Fe cannot be overlooked in this region. Unfortunately, CLE-CSV does not distinguish between inorganic and organic ligands, however nanosized colloids (including illite, goethite and hematite) likely comprise a fraction of FeL in seawater here (Petschick et al., 1996; van der Zee et al., 2003; Homoky et al., 2021) due to subglacial plumes and sediment resuspension at the shelf (Harris and Beaman, 2003; Raiswell et al., 2018; Forsch et al., 2021). As FeL concentrations were greatest at depth, a combination of these sources likely supplies surface waters with complexed Fe through vertical mixing, which supports primary production in late summer.

3.5 The Mertz Region and Southern Ocean Ligand Collection

As reference materials are scarce for complexation studies, comparisons between the methods and data of previous studies in similar regions is our best available tool for intercalibration of past datasets. To compare data from the ENRICH survey of the Mertz Glacier Region with other studies we compiled 25 datasets from Southern Ocean Fe complexation studies in the SOLt Collection. Building upon previous work by Caprara et al. (2016), this collection now includes 1,072 samples collected between 21st March 1995 – 26th February 2019 (most recently, this study). The SOLt Collection is available to download from the IMAS Metadata Catalogue (https://metadata.imas.utas.edu.au/).

Within the SOLt Collection sampling period varied seasonally with 65% of studies performed during austral summer (December – February, Figure 6A). To date, heavy emphasis has been placed on sampling the Pacific sector of the Southern Ocean, between the Ross Sea and Western Antarctic Peninsula. Very little data was available for the west Indian Ocean between 30 – 70°E. Studies were evenly distributed between small-scale transects (< 1,000 km, 32%), large-scale transects (> 1,000 km, 32%) and process or experimental studies (36%).

Total ligand concentrations from the Mertz Region determined in the ENRICH study were within the bounds of concentrations observed in other Southern Ocean complexation studies (0.17 – 15.7 nM Eq Fe, Table 1). High concentrations of L' (estimated as Lt – dFe) were visible below 100 m in the SOLt Collection indicating that while microbial production is attributed to excess L' concentrations in many studies (Table 1), L' supplied from depth (via over-turning, upwelling or vertical mixing) may also contribute to high Lt:dFe ratios. As our complexation data to date is dominated by studies performed in austral summer months (Figure 6A) when the water column is typically stratified, we lack complexation data from winter months (May – September) when vertical mixing is enhanced (Tagliabue et al., 2014) and L' are brought from depth to towards surface waters. Moreover, strong ligands in the SOLt Collection were detected at higher latitudes in deeper waters (> 100 m, $R^2 = 0.05$, $P = 3.85 \times 10^{-7}$, Figure 6B), suggesting that shelf productivity and sediments influence ligand binding strength near the Antarctic continent.

Across the Collection, the greatest Lt concentration recorded was during the Antarctic Circumnavigation Expedition (ACE, Hassler et al., 2020a). This value was reported for seawater collected from 75 m depth at a station 44 km west of the Balleny Islands. The ACE survey area overlapped the ENRICH survey area within the Mertz Region. Although over a similar sampling period to the ENRICH survey (January – February), Lt concentrations from the ACE survey were 3 times greater, and

TABLE 1 Overview of complexation results and methods used in the Southern Ocean Ligand (SOLt) Collection including dissolved iron (dFe), Fe-binding ligand concentration (Lt) and conditional stability constants (Log K_{FeL} and Log $K_{Fe'}$, depending on side reaction coefficient used in calculation).

Location	AL	dFe (nM)	Lt (nM Eq Fe)	Log K_{FeL}	Log $K_{Fe'}$	Suggested ligand source	Study
Amundsen Sea	TAC	0.042 - 1.31	0.04 - 0.88	21 - 23		Upwelling near shelf and blooms	Thuróczy et al., 2012
Atlantic Sector Southern Ocean	TAC & NN	0.2 - 0.5	1.7 - 3.0	21.7 - 22.7		Biological source (DCM)	Croot et al., 2004
	TAC	0.06 - 0.09	0.60 - 0.79	21.7 - 22.2		Unreported	Boye et al., 2005
	TAC	0.04 - 0.41	0.58 - 0.86	21.0 - 22.9		Biological source (DCM) and regeneration of sinking particles	Boye et al., 2010
	TAC	0.02 - 0.59	0.54 - 1.84	21 - 22		Unreported	Thuróczy et al., 2011
	SA	0.22	0.99		11.3	Unreported	Cabanes et al., 2017
	DHN	0.17 - 1.29	1.2 - 3.7		11.2 - 12.5	Sloppy feeding by grazers, phytoplankton exudation	Laglera et al., 2020
Chatham Rise, New Zealand	TAC	0.07 - 0.29	0.66 - 1.16	22.5 - 22.9		Regional currents & upwelling	Tian et al., 2006
Kerguelen Plateau	TAC	0.05 - 0.39	0.17 - 1.61	21.0 - 22.8		Phytoplankton & sediment	Gerringa et al., 2008
	TAC	0.05 - 0.76	0.26 - 2.63	20.2 - 22.4		Large diatoms and bacterial remineralisation	Tonnard, 2018
Mertz Region	TAC	0.03 - 0.6	0.18 - 2.78	20.3 - 26.9		Deep water upwelling, sediments, and remineralisation by bacteria	*This study*
	SA	0.01 – 0.59	0.41 - 15.7		10.2 - 12.4	Unreported	Hassler et al., 2020a
Pacific Sector Southern Ocean	NN	0.21 - 0.72	2 - 12	20.6 -21.6		Hydrography (upwelling water masses)	Nolting et al., 1998
	TAC	0.17 - 0.67	0.56 - 1.31		11.7 - 12.5	Biological source (DCM)	Kondo et al., 2012
Ross Sea	DHN	0.52 - 5.41	1.4 - 8		12.1 - 12.6	Biological source (DCM)	Rivaro et al., 2019
	TAC	0.012 - 2.34	0.31 - 2.61		11.6 - 13.4	Biological source (DCM)	Gerringa et al., 2020
Subantarctic zone	TAC	0.22 - 0.27	0.32 - 0.49	22.5 - 23.6		Siderophores produced by bacterioplankton	Ibisanmi et al., 2011
	TAC	0.14	0.65		11.2	Unreported	Bressac et al., 2019
	TAC	0.2 - 1	0.7 - 1.3	22 - 23		Siderophores, humic acids	Sander et al., 2015
Under fast ice: East Antarctica	NN	1.5 - 3.7	4.9 - 9.6	21.2 - 22.1		Microbial origin within sea-ice	Lannuzel et al., 2015
West Indian Sector of Southern Ocean	NN	0.1 - 0.6	<0.18 – 1.39	21.6 - 22.6		Microorganisms. Loss to photodegradation in surface	Boye et al., 2001
	TAC	0.08 - 0.97	0.71 - 3.34			Vertical mixing and phytoplankton/bacteria release	Schlosser et al., 2012
Western Antarctic Peninsula	SA	0.34 - 0.74	1.12 - 1.67		11.3 -11.7	Unreported	Cabanes et al., 2020
	SA	0.29 - 2.26	1.23 - 6.43		10 - 12.4	Surface: Phytoplankton exudates and sea-ice. Depth: Sediments & Upwelling	Ardiningsih et al., 2021a
	TAC	1.13 - 1.307	1.6		11.6	Unreported	Böckmann et al., 2021

The table is arranged by sampling location and year published. Artificial ligands (AL) used in CLE-CSV analyses include 2-(2-thiazolylazo)-*p*-cresol (TAC), 1-nitroso-2-napthol (NN), salicylaldoxime (SA) and 2,3-dihydroxynaphtalene (DHN).

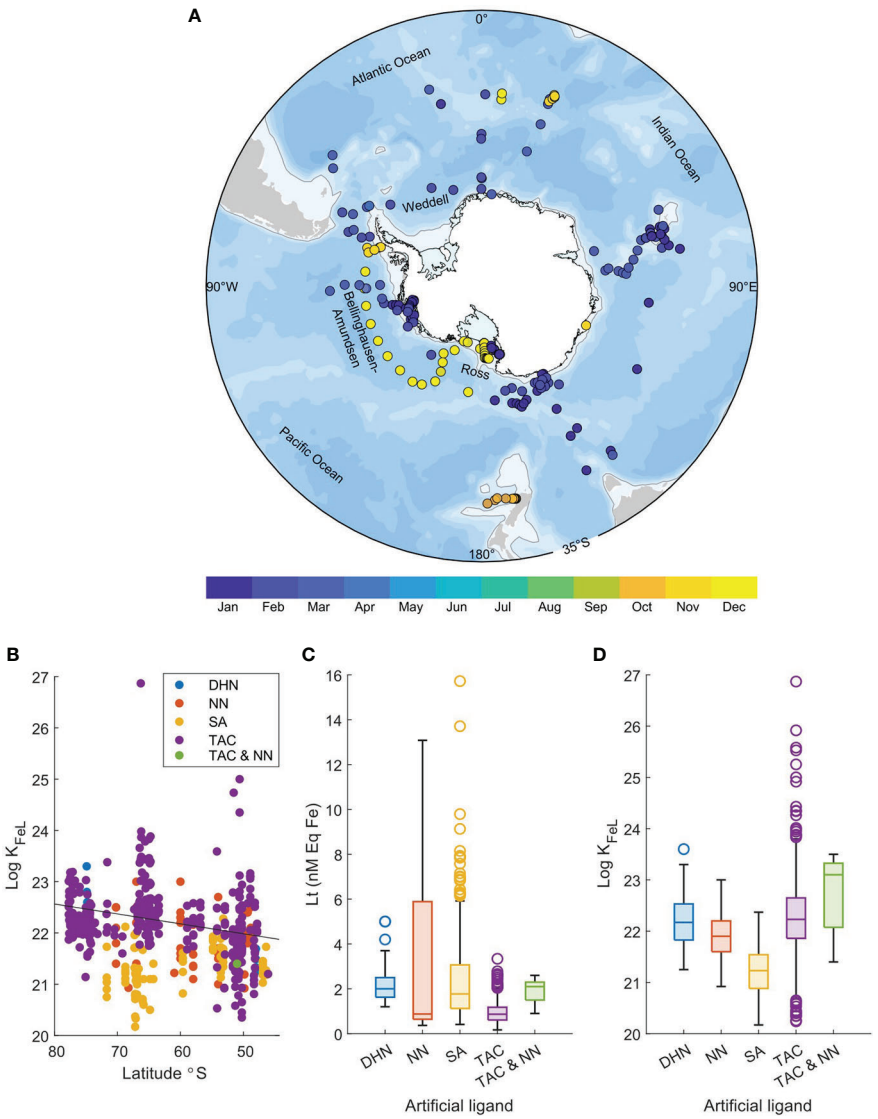

FIGURE 6
(A) Seasonal distribution of stations included in the Southern Ocean Ligand Collection. Colour bar represents sampling month. **(B)** Relationship between Log K_{FeL} and latitude (°S) for deep samples collected >100 m, coloured by artificial ligand used, including 2-(2-thiazolylazo)-*p*-cresol (TAC), 1-nitroso-2-napthol (NN), salicylaldoxime (SA) and 2,3-dihydroxynaphtalene (DHN). Box-and-Whisker plot of **(C)** Lt concentration (nM Eq Fe) and **(D)** Log K_{FeL} with different artificial ligand methods.

correspondingly Log K values were smaller than those collected from ENRICH. While ACE sampling stations were closer to the base of the Mertz Glacier than those of ENRICH, complexation data from the ACE study was determined using SA (5 μM) as the competing ligand, which is presently thought to be the most reliable CLE-CSV method for seawater (Abualhaija and van den Berg, 2014; Gerringa et al., 2021).

The five artificial ligand methods used in the SOLt Collection yield significantly variable estimates of Lt (Figure 6B) and Log K_{FeL} (Figure 6C, ANOVA, $P < 2.2 \times 10^{-16}$, df = 4). Elevated concentrations of Lt are observed when SA and NN are used, whereas increased Log K_{FeL} values were recorded for studies using TAC (Figure 6D, irrespective of high values recorded during the ENRICH survey). Such observations have also been made in the Arctic (Ardiningsih et al., 2021b) and conditional stability constants have been noted to only provide a rough estimate of binding strength (Gerringa et al., 2021) which varies with salinity, temperature, and pH, depending on the selected method (Genovese et al., 2022). Therefore, understanding whether trends between Fe-binding ligands and environmental

variables are linked to true seasonal supply mechanisms or analytical variability will be crucial to complexation studies going forward.

Intercalibration exercises are rare for CLE-AdCSV analyses, due to a lack of reproducible and well-preserved reference materials (Buck et al., 2012; Pižeta et al., 2015; Buck et al., 2016; Lauderdale et al., 2020). Formally reviewed intercalibration reports present opportunities to compile standardized ligand datasets globally. For example, reports generated by the GEOTRACES Intermediate Data Product (IDP) require detailed descriptions of the voltammetric and modelling techniques used, data quality control, and descriptions of reference samples or cross-over stations, if available (GEOTRACES Intermediate Data Product Group, 2021). Croot et al. (2004) compared results from two AL methods (NN and TAC) simultaneously to produce a robust assessment of ligand concentration. This approach increased confidence in the results, but it also dramatically increased the analytical cost, time and volume of seawater sample required. Therefore, this may not be feasible for large sample quantities that are typically collected from Southern Ocean voyages. Recent developments to CLE-CSV methods show sample volume and analytical time could be reduced substantially (i.e., 15 mL sample measured in 30 minutes, rather than 125mL sample measured in 6 hours) without compromising on trace level detection limits (Sanvito and Monticelli, 2020). This could boost our ability to measure ligands in the Southern Ocean.

Due to the remote location and seasonal challenges associated with collecting Southern Ocean samples, clear gaps emerge along the East Antarctic coastline, with the later summer months largely under-sampled. Across the studies to date, suggested Lt inputs range from lithogenic to biogenic sources, with the sparsity of data preventing clear attribution of driver(s) to complexation. As with trace element concentrations, there is a need for repeat basin-scale transects to assess how ligands are distributed with latitude and across oceanographic fronts, and how this distribution changes as the season progresses. Seasonal process studies near continental or sea-ice melt (such as the Marginal Ice Zone) will allow us to capture the physical supply of Fe and ligands, in addition to the onset of spring blooms and subsequent biological depletion of resources. Additional parameters, including dissolved and particulate organic carbon, transparent exopolymeric particles (TEPs), and determination of ligand molecular structure via organic mass spectrometry (Rivaro et al., 2021), would benefit the identification of ligands from biological sources. Assessment of seafloor sediments to Fe and ligand supply requires collection of pore water samples for CLE-AdCSV analysis and measurements of diffusion and seawater movement at the seawater-sediment interface (i.e., Forsch et al., 2021). Humic or fulvic acid fluorescence (Tani et al., 2003; Heller et al., 2013) offers an efficient method to assess HS or HS-like molecules and aid identification of HS sources to the ligand pool. Increased spatial and seasonal sampling of Southern Ocean ligands, coupled with key environmental drivers known to influence supply, will strengthen our ability to identify which processes influence Fe availability and how sensitive these processes are to future environmental change.

4 Conclusions

Processes that drive primary productivity are subject to environmental changes, therefore constraining Fe complexation and thus availability to primary producers is central to our understanding of the future Southern Ocean. In our study, strong binding ligands complexed Fe in the Mertz Glacier Region during late summer. Iron and ligands were most likely supplied from deep sources such as upwelled CDW and remineralization of suspended particles in benthic nepheloid layers. The strongest Fe-binding ligands observed were in mCDW where microbial remineralization was identified, alluding to siderophore production at depth. Photo-degradation of FeL appeared to increase concentrations of L' and Fe' in surface waters, and phytoplankton consumption of Fe likely led to excess L', which rapidly complexes new additions of Fe. Recent sea-ice melt was associated with low Fe complexation, contradicting previous studies where high concentrations of FeL were measured in sea ice. Elevated bacterial production near sea-ice melt may have been in response to Fe released earlier in the season. The SOLt Collection highlighted analytical differences in CLE-CSV methods across Southern Ocean Fe-binding ligand surveys, requiring improvement through intercalibration procedures. It also identified key gaps in spatial and temporal coverage of Southern Ocean complexation research.

Data availability statement

The datasets presented in this study can be found in online repositories. The names of the repository/repositories and accession number(s) can be found below: (https://metadata.imas.utas.edu.au/).

Author contributions

AS, LR, TH, TN were responsible for the collection and analysis of trace element samples. AS, TN, CG, AT and KWu critically revised the ligand data. KWe was responsible for bacterial production data. MC was responsible for sea ice satellite data interpretations and mapping. AS compiled the SOLt Collection, interpreted the analyses and drafted the manuscript. TN, LR, CG, KWe, TH, MC, AT, EB, KW and DL

equally contributed to editing and revisions of this manuscript. All authors contributed to the article and approved the submitted version.

Funding

Antarctic research on the ENRICH voyage was permitted under the Notice of Determination and Authorization for the Antarctic Treaty (Environment Protection) Act 1980 issued by the Australian Antarctic Division (AAD) on 27 September 2018. This work was conducted as part of the Australian Antarctic Program under Australian Antarctic Science (AAS) Project 4101—Antarctic baleen whale habitat utilization and linkages to environmental characteristics and/or AAS Project 4102—Population abundance, trend, structure and distribution of the endangered Antarctic blue whale, and/or AAS Project 4600—Conservation and management of Australian and Antarctic whales – post-exploitation status, distribution, foraging ecology and their role in the Southern Ocean ecosystem and/or AAS Project 4512—Ensuring sustainable management of the krill fishery in waters off the Australian Antarctic Territory. LR received support from BYONIC (ERC award number 724289). DL is funded by the Australian Research Council (ARC Future Fellowship L0026677). Access to SF-ICP-MS instrumentation was made possible by an Australian Research Council grant (LE0989539).

Acknowledgments

The authors are indebted to the Australian Antarctic Division (AAD) for their support in funding, organization, and development of this research and to the CSIRO Marine National Facility (MNF) for its support in the form of sea time on RV *Investigator*, support personnel, scientific equipment, and data management. The authors are grateful to the ENRICH voyage Chief Scientists Mike Double, Elanor Bell and Brian Miller, as well as all participants of the voyage. We wish to thank Nat Kelly for designing the ENRICH survey to facilitate biogeochemical sampling, as well as Steve Nicol and Loes Gerringa for their helpful discussions of this research. We also wish to thank Madeleine Brasier, James O'Brien and Clara Rodrigues Vives for undertaking physical and biological oceanography measurements. Analyses and visualizations used in this paper were produced with the Giovanni online data system, developed, and maintained by the NASA GES DISC. Data was sourced from Australia's Integrated Marine Observing System (IMOS) – IMOS is enabled by the National Collaborative Research Infrastructure strategy (NCRIS). It is operated by a consortium of institutions as an unincorporated joint venture, with the University of Tasmania as Lead Agent.

Conflict of interest

The authors declare that the research was conducted in the absence of any commercial or financial relationships that could be construed as a potential conflict of interest.

Publisher's note

All claims expressed in this article are solely those of the authors and do not necessarily represent those of their affiliated organizations, or those of the publisher, the editors and the reviewers. Any product that may be evaluated in this article, or claim that may be made by its manufacturer, is not guaranteed or endorsed by the publisher.

Supplementary material

The Supplementary Material for this article can be found online at: https://www.frontiersin.org/articles/10.3389/fmars.2022.948772/full#supplementary-material

References

Abualhaija, M. M., and van den Berg, C. M. G. (2014). Chemical speciation of iron in seawater using catalytic cathodic stripping voltammetry with ligand competition against salicylaldoxime. *Mar. Chem.* 164, 60–74. doi: 10.1016/j.marchem.2014.06.005

Ardiningsih, I., Seyitmuhammedov, K., Sander, S. G., Stirling, C. H., Reichart, G. J., Arrigo, K. R., et al. (2021a). Fe-binding organic ligands in coastal and frontal regions of the western Antarctic peninsula. *Biogeosciences* 18, 4587–4601. doi: 10.5194/bg-18-4587-2021

Ardiningsih, I., Zhu, K., Lodeiro, P., Gledhill, M., Reichart, G.-J., Achterberg, E. P., et al. (2021b). Iron speciation in fram strait and over the northeast Greenland shelf: An inter-comparison study of voltammetric methods. *Front. Mar. Sci.* 7. doi: 10.3389/fmars.2020.609379

Biggs, T. E. G., Huisman, J., and Brussaard, C. P. D. (2021). Viral lysis modifies seasonal phytoplankton dynamics and carbon flow in the southern ocean. *ISME J.* 15, 3615–3622. doi: 10.1038/s41396-021-01033-6

Bindoff, N., Rintoul, S. R., and Massom, R. A. (2000). Bottom water formation and polynyas in Adelie Land, Antarctica. *Papers and Proceedings of the Royal Society of Tasmania* 133, 51–56.

Böckmann, S., Koch, F., Meyer, B., Pausch, F., Iversen, M., Driscoll, R., et al. (2021). Salp fecal pellets release more bioavailable iron to southern ocean phytoplankton than krill fecal pellets. *Curr. Biol.* 31, 2737–2746. doi: 10.1016/j.cub.2021.02.033

Boiteau, R. M., Mende, D. R., Hawco, N. J., McIlvin, M. R., Fitzsimmons, J. N., Saito, M. A., et al. (2016). Siderophore-based microbial adaptations to iron scarcity

across the eastern pacific ocean. *Proc. Natl. Acad. Sci. U.S.A.* 113, 14237–14242. doi: 10.1073/pnas.1608594113

Bowman, J. P. (2013). "Sea-Ice microbial communities," in *The prokaryotes: Prokaryotic communities and ecophysiology*. Eds. E. Rosenberg, E. F. DeLong, S. Lory, E. Stackebrandt and F. Thompson (Berlin Heidelberg: Springer), 139–161.

Boyd, P. W., and Ellwood, M. J. (2010). The biogeochemical cycle of iron in the ocean. *Nat. Geosci.* 3, 675. doi: 10.1038/ngeo964

Boyd, P. W., Jickells, T., Law, C. S., Blain, S., Boyle, E. A., Buesseler, K. O., et al. (2007). Mesoscale iron enrichment experiments 1993-2005: Synthesis and future directions. *Science* 315, 612–617. doi: 10.1126/science.1131669

Boyd, P. W., Strzepek, R., Chiswell, S., Chang, H., DeBruyn, J. M., Ellwood, M., et al. (2012). Microbial control of diatom bloom dynamics in the open ocean. *Geophysical Res. Lett.* 39, 1–6. doi: 10.1029/2012GL053448

Boye, M., Nishioka, J., Croot, P. L., Laan, P., Timmermans, K. R., and de Baar, H. J. W. (2005). Major deviations of iron complexation during 22 days of a mesoscale iron enrichment in the open southern ocean. *Mar. Chem.* 96, 257–271. doi: 10.1016/j.marchem.2005.02.002

Boye, M., Nishioka, J., Croot, P., Laan, P., Timmermans, K. R., Strass, V. H., et al. (2010). Significant portion of dissolved organic fe complexes in fact is fe colloids. *Mar. Chem.* 122, 20–27. doi: 10.1016/j.marchem.2010.09.001

Boye, M., van den Berg, C. M. G., de Jong, J. T. M., Leach, H., Croot, P., and de Baar, H. J. W. (2001). Organic complexation of iron in the southern ocean. *Deep Sea Res. Part I: Oceanogr. Res. Papers* 48, 1477–1497. doi: 10.1016/S0967-0637(00)00099-6

Bressac, M., Guieu, C., Ellwood, M. J., Tagliabue, A., Wagener, T., Laurenceau-Cornec, E. C., et al. (2019). Resupply of mesopelagic dissolved iron controlled by particulate iron composition. *Nat. Geosci.* 12, 995–1000. doi: 10.1038/s41561-019-0476-6

Buck, K. N., Gerringa, L. J. A., and Rijkenberg, M. J. A. (2016). An intercomparison of dissolved iron speciation at the Bermuda Atlantic time-series study (BATS) site: Results from GEOTRACES crossover station a. *Front. Mar. Sci.* 3. doi: 10.3389/fmars.2016.00262

Buck, K. N., Moffett, J., Barbeau, K. A., Bundy, R. M., Kondo, Y., and Wu, J. (2012). The organic complexation of iron and copper: an intercomparison of competitive ligand exchange-adsorptive cathodic stripping voltammetry (CLE-ACSV) techniques. *Limnology Oceanogr.: Methods* 10, 496–515. doi: 10.4319/lom.2012.10.496

Buck, K. N., Sedwick, P. N., Sohst, B., and Carlson, C. A. (2018). Organic complexation of iron in the eastern tropical South Pacific: Results from US GEOTRACES Eastern Pacific Zonal Transect (GEOTRACES cruise GP16). *Marine Chemistry* 201, 229–241.

Buck, K. N., Sohst, B., and Sedwick, P. N. (2015). The organic complexation of dissolved iron along the U.S. GEOTRACES (GA03) north Atlantic section. *Deep Sea Res. Part II: Topical Stud. Oceanogr.* 116, 152–165. doi: 10.1016/j.dsr2.2014.11.016

Bundy, R. M., Biller, D. V., Buck, K. N., Bruland, K. W., and Barbeau, K. A. (2014). Distinct pools of dissolved iron-binding ligands in the surface and benthic boundary layer of the California current. *Limnology Oceanogr.* 59, 769–787. doi: 10.4319/lo.2014.59.3.0769

Bundy, R. M., Jiang, M., Carter, M., and Barbeau, K. A. (2016). Iron-binding ligands in the southern California current system: Mechanistic studies. *Front. Mar. Sci.* 3. doi: 10.3389/fmars.2016.00027

Cabanes, D. J. E., Blanco-Ameijeiras, S., Bergin, K., Trimborn, S., Völkner, C., Lelchat, F., et al. (2020). Using fe chemistry to predict fe uptake rates for natural plankton assemblages from the southern ocean. *Mar. Chem.* 225, 103853. doi: 10.1016/j.marchem.2020.103853

Cabanes, D. J. E., Norman, L., Santos-Echeandía, J., Iversen, M. H., Trimborn, S., Laglera, L. M., et al. (2017). First evaluation of the role of salp fecal pellets on iron biogeochemistry. *Front. Mar. Sci.* 3. doi: 10.3389/fmars.2016.00289

Calace, N., Casagrande, A., Mirante, S., Petronio, B. M., and Pietroletti, M. (2010). Distribution of humic substances dissolved and particulated in water column in Ross Sea, Antarctica. *Microchemical J.* 96, 218–224. doi: 10.1016/j.microc.2009.07.005

Caprara, S., Buck, K. N., Gerringa, L. J. A., Rijkenberg, M. J. A., and Monticelli, D. (2016). A compilation of iron speciation data for open oceanic waters. *Front. Mar. Sci.* 3. doi: 10.3389/fmars.2016.00221

Carter, L., McCave, I. N., and Williams, M. J. M. (2008). "Chapter 4 circulation and water masses of the southern ocean: A review," in *Developments in earth and environmental sciences*. Eds. F. Florindo and M. Siegert (Amsterdam, Netherland: Elsevier), 85–114.

Cougnon, E. A., Galton-Fenzi, B. K., Meijers, A. J. S., and Legrésy, B. (2013). Modeling interannual dense shelf water export in the region of the mertz glacier tongue(1992–2007). *J. Geophysical Research: Oceans* 118, 5858–5872. doi: 10.1002/2013JC008790

Croot, P. L., Andersson, K., Öztürk, M., and Turner, D. R. (2004). The distribution and speciation of iron along 6°E in the southern ocean. *Deep Sea Res. Part II: Topical Stud. Oceanogr.* 51, 2857–2879. doi: 10.1016/j.dsr2.2003.10.012

Croot, P., and Heller, M. (2012). The importance of kinetics and redox in the biogeochemical cycling of iron in the surface ocean. *Front. Microbiol.* 3. doi: 10.3389/fmicb.2012.00219

Croot, P. L., and Johansson, M. (2000). Determination of iron speciation by cathodic stripping voltammetry in seawater using the competing ligand 2-(2-Thiazolylazo)-*p*-cresol (TAC). *Electroanalysis* 12, 565–576. doi: 10.1002/(SICI)1521-4109(200005)12:8<565::AID-ELAN565>3.0.CO;2-L

Cunningham, K. M., Goldberg, M. C., and Weiner, E. R. (1988). Mechanisms for aqueous photolysis of adsorbed benzoate, oxalate, and succinate on iron oxyhydroxide (goethite) surfaces. *Environ. Sci. Technol.* 22, 1090–1097. doi: 10.1021/es00174a015

Cutter, G., Casciotti, K., Croot, P., Geibert, W., Heimbürger, L.-E., Lohan, M., et al. (2017). *Sampling and Sample-handling Protocols for GEOTRACES Cruises. Version 3*. Toulouse, France: GEOTRACES International Project Office, 139. doi: 10.25607/OBP-2

Death, R., Wadham, J. L., Monteiro, F., Le Brocq, A. M., Tranter, M., Ridgwell, A., et al. (2014). Antarctic Ice sheet fertilises the southern ocean. *Biogeosciences* 11, 2635–2643. doi: 10.5194/bg-11-2635-2014

de Boyer Montégut, C., Madec, G., Fischer, A. S., Lazar, A., and Iudicone, D. (2004). Mixed layer depth over the global ocean: An examination of profile data and a profile-based climatology. *J. Geophysical Research: Oceans* 109, 1–20. doi: 10.1029/2004jc002378

Dinniman, M. S., St-Laurent, P., Arrigo, K. R., Hofmann, E. E., and van Dijken, G. L. (2020). Analysis of iron sources in Antarctic continental shelf waters. *J. Geophysical Research: Oceans* 125, e2019JC015736. doi: 10.1029/2019jc015736

Eayrs, C., Holland, D., Francis, D., Wagner, T., Kumar, R., and Li, X. (2019). Understanding the seasonal cycle of Antarctic Sea ice extent in the context of longer-term variability. *Rev. Geophysics* 57, 1037–1064. doi: 10.1029/2018RG000631

England, M. H. (1995). he Age of Water and Ventilation Timescales in a Global Ocean Model. *J. Phys. Oceanogr.* 25, 2756–2777. doi: 10.1175/1520-0485(1995)025<2756:TAOWAV>2.0.CO;2

Forsch, K. O., Hahn-Woernle, L., Sherrell, R. M., Roccanova, V. J., Bu, K., Burdige, D., et al. (2021). Seasonal dispersal of fjord meltwaters as an important source of iron and manganese to coastal Antarctic phytoplankton. *Biogeosciences* 18, 6349–6375. doi: 10.5194/bg-18-6349-2021

Gardner, W. D., Richardson, M. J., and Mishonov, A. V. (2018). Global assessment of benthic nepheloid layers and linkage with upper ocean dynamics. *Earth Planetary Sci. Lett.* 482, 126–134. doi: 10.1016/j.epsl.2017.11.008

Genovese, C., Grotti, M., Ardini, F., Wuttig, K., Vivado, D., Cabanes, D., et al. (2022). Effect of salinity and temperature on the determination of dissolved iron-binding organic ligands in the polar marine environment. *Mar. Chem.* 238, 104051. doi: 10.1016/j.marchem.2021.104051

Genovese, C., Grotti, M., Pittaluga, J., Ardini, F., Janssens, J., Wuttig, K., et al. (2018). Influence of organic complexation on dissolved iron distribution in East Antarctic pack ice. *Mar. Chem.* 203, 28–37. doi: 10.1016/j.marchem.2018.04.005

GEOTRACES Intermediate Data Product Group (2021). The GEOTRACES Intermediate Data Product 2021 (IDP2021). *NERC EDS British Oceanographic Data Centre NOC*. doi: 10.5285/cf2d9ba9-d51d-3b7c-e053-8486abc0f5fd

Gerringa, L. J. A., Alderkamp, A.-C., van Dijken, G., Laan, P., Middag, R., and Arrigo, K. R. (2020). Dissolved trace metals in the Ross Sea. *Front. Mar. Sci.* 7. doi: 10.3389/fmars.2020.577098

Gerringa, L. J. A., Blain, S., Laan, P., Sarthou, G., Veldhuis, M. J. W., Brussaard, C. P. D., et al. (2008). Fe-binding dissolved organic ligands near the kerguelen archipelago in the southern ocean (Indian sector). *Deep Sea Res. Part II: Topical Stud. Oceanogr.* 55, 606–621. doi: 10.1016/j.dsr2.2007.12.007

Gerringa, L. J. A., Gledhill, M., Ardiningsih, I., Muntjewerf, N., and Laglera, L. M. (2021). Comparing CLE-AdCSV applications using SA and TAC to determine the fe-binding characteristics of model ligands in seawater. *Biogeosciences* 18, 5265–5289. doi: 10.5194/bg-18-5265-2021

Gerringa, L. J. A., Rijkenberg, M. J. A., Schoemann, V., Laan, P., and de Baar, H. J. W. (2015). Organic complexation of iron in the West Atlantic ocean. *Mar. Chem.* 177, 434–446. doi: 10.1016/j.marchem.2015.04.007

Gledhill, M., and Buck, K. (2012). The organic complexation of iron in the marine environment: A review. *Front. Microbiol.* 3. doi: 10.3389/fmicb.2012.00069

Gledhill, M., McCormack, P., Ussher, S., Achterberg, E. P., Mantoura, R. F. C., and Worsfold, P. J. (2004). Production of siderophore type chelates by mixed bacterioplankton populations in nutrient enriched seawater incubations. *Mar. Chem.* 88, 75–83. doi: 10.1016/j.marchem.2004.03.003

Graham, R. M., De Boer, A. M., Van Sebille, E., Kohfeld, K. E., and Schlosser, C. (2015). Inferring source regions and supply mechanisms of iron in the southern

ocean from satellite chlorophyll data. *Deep Sea Res. Part I: Oceanogr. Res. Papers* 104, 9–25. doi: 10.1016/j.dsr.2015.05.007

Harris, P. T., and Beaman, R. J. (2003). Processes controlling the formation of the mertz drift, George vth continental shelf, East Antarctica: evidence from 3.5kHz sub-bottom profiling and sediment cores. *Deep Sea Res. Part II: Topical Stud. Oceanogr.* 50, 1463–1480. doi: 10.1016/S0967-0645(03)00070-5

Hassler, C., Cabanes, D. J. E., Blanco-Ameijeiras, S., Sander, S. G., and Benner, R. (2020b). Importance of refractory ligands and their photodegradation for iron oceanic inventories and cycling. *Mar. Freshw. Res.* 71, 311–320. doi: 10.1071/MF19213

Hassler, C., Cabanes, D., Ellwood, M., Conway, T., and Sieber, M. (2020a). *Fe chemical speciation collected using trace metal rosette in the southern ocean during the austral summer of 2016/2017, on board the Antarctic circumnavigation expedition* (Zenodo). (Dataset).

Hassler, C. S., Schoemann, V., Nichols, C. M., Butler, E. C. V., and Boyd, P. W. (2011). Saccharides enhance iron bioavailability to southern ocean phytoplankton. *Proc. Natl. Acad. Sci.*,108 1076–1081. doi: 10.1073/pnas.1010963108

Hassler, C. S., van den Berg, C. M. G., and Boyd, P. W. (2017). Toward a regional classification to provide a more inclusive examination of the ocean biogeochemistry of iron-binding ligands. *Front. Mar. Sci.* 4. doi: 10.3389/fmars.2017.00019

Heller, M. I., Gaiero, D. M., and Croot, P. L. (2013). Basin scale survey of marine humic fluorescence in the Atlantic: Relationship to iron solubility and H_2O_2. *Global Biogeochem. Cycles* 27, 88–100. doi: 10.1029/2012GB004427

Hogle, S. L., Dupont, C. L., Hopkinson, B. M., King, A. L., Buck, K. N., Roe, K. L., et al. (2018). Pervasive iron limitation at subsurface chlorophyll maxima of the California current. *Proc. Natl. Acad. Sci.* 115, 13300–13305. doi: 10.1073/pnas.1813192115

Holmes, T. M., Wuttig, K., Chase, Z., Schallenberg, C., van der Merwe, P., Townsend, A. T., et al. (2020). Glacial and hydrothermal sources of dissolved iron (II) in southern ocean waters surrounding heard and McDonald islands. *J. Geophysical Research: Oceans* 125, e2020JC016286. doi: 10.1029/2020JC016286

Homoky, W. B., Conway, T. M., John, S. G., König, D., Deng, F., Tagliabue, A., et al. (2021). Iron colloids dominate sedimentary supply to the ocean interior. *Proc. Natl. Acad. Sci.* 118, e2016078118. doi: 10.1073/pnas.2016078118

Hutchins, D. A., Witter, A. E., Butler, A., and Luther, G. W. (1999). Competition among marine phytoplankton for different chelated iron species. *Nature* 400, 858–861. doi: 10.1038/23680

Ibisanmi, E., Sander, S. G., Boyd, P. W., Bowie, A. R., and Hunter, K. A. (2011). Vertical distributions of iron-(III) complexing ligands in the southern ocean. *Deep Sea Res. Part II: Topical Stud. Oceanogr.* 58, 2113–2125. doi: 10.1016/j.dsr2.2011.05.028

Janssen, D. J., Sieber, M., Ellwood, M. J., Conway, T. M., Barrett, P. M., Chen, X., et al. (2020). Trace metal and nutrient dynamics across broad biogeochemical gradients in the Indian and pacific sectors of the southern ocean. *Mar. Chem.* 221, 103773. doi: 10.1016/j.marchem.2020.103773

Janssens, J., Meiners, K. M., Townsend, A. T., and Lannuzel, D. (2018). Organic matter controls of iron incorporation in growing sea ice. *Front. Earth Sci.* 6. doi: 10.3389/feart.2018.00022

Jardon, F. P., Vivier, F., Vancoppenolle, M., Lourenço, A., Bouruet-Aubertot, P., and Cuypers, Y. (2013). Full-depth desalination of warm sea ice. *J. Geophysical Research: Oceans* 118, 435–447. doi: 10.1029/2012JC007962

Johnson, K. S., Gordon, R. M., and Coale, K. H. (1997). What controls dissolved iron concentrations in the world ocean? *Mar. Chem.* 57, 137–161. doi: 10.1016/S0304-4203(97)00043-1

Kirchman, D. L., Meon, B., Cottrell, M. T., Hutchins, D. A., Weeks, D., and Bruland, K. W. (2000). Carbon versus iron limitation of bacterial growth in the California upwelling regime. *Limnology Oceanogr.* 45, 1681–1688. doi: 10.4319/lo.2000.45.8.1681

Kondo, Y., Takeda, S., and Furuya, K. (2012). Distinct trends in dissolved fe speciation between shallow and deep waters in the pacific ocean. *Mar. Chem.* 134-135, 18–28. doi: 10.1016/j.marchem.2012.03.002

Laglera, L. M., Battaglia, G., and van den Berg, C. M. G. (2011). Effect of humic substances on the iron speciation in natural waters by CLE/CSV. *Mar. Chem.* 127, 134–143. doi: 10.1016/j.marchem.2011.09.003

Laglera, L. M., Tovar-Sanchez, A., Sukekava, C., Naik, H., Naqvi, S., and Wolf-Gladrow, D. (2020). Iron organic speciation during the LOHAFEX experiment: Iron ligands release under biomass control by copepod grazing. *J. Mar. Syst.* 207, 103151. doi: 10.1016/j.jmarsys.2019.02.002

Laglera, L. M., and van den Berg, C. M. (2009). Evidence for geochemical control of iron by humic substances in seawater. *Limnology Oceanogr.* 54, 610–619. doi: 10.4319/lo.2009.54.2.0610

Lannuzel, D., Grotti, M., Abelmoschi, M. L., and van der Merwe, P. (2015). Organic ligands control the concentrations of dissolved iron in Antarctic sea ice. *Mar. Chem.* 174, 120–130. doi: 10.1016/j.marchem.2015.05.005

Lannuzel, D., Vancoppenolle, M., van der Merwe, P., De Jong, J., Meiners, K. M., Grotti, M., et al. (2016). Iron in sea ice: Review and new insights. *Elem. Sci. Anth.* 4, 1–19. doi: 10.12952/journal.elementa.000130

Lauderdale, J. M., Braakman, R., Forget, G., Dutkiewicz, S., and Follows, M. J. (2020). Microbial feedbacks optimize ocean iron availability. *Proc. Natl. Acad. Sci.* 117, 4842–4849. doi: 10.1073/pnas.1917277117

Lehmann, M. K., Davis, R. F., Huot, Y., and Cullen, J. J. (2004). Spectrally weighted transparency in models of water-column photosynthesis and photoinhibition by ultraviolet radiation. *Mar. Ecol. Prog. Ser.* 269, 101–110. doi: 10.3354/meps269101

Liniger, G., Strutton, P. G., Lannuzel, D., and Moreau, S. (2020). Calving event led to changes in phytoplankton bloom phenology in the mertz polynya, Antarctica. *J. Geophysical Research: Oceans* 125, e2020JC016387. doi: 10.1029/2020JC016387

Martin, J. H., Gordon, R. M., and Fitzwater, S. E. (1990). Iron in Antarctic waters. *Nature* 345, 156–58. doi: 10.1038/345156a0

Matsumoto, K. (2007). Radiocarbon-based circulation age of the world oceans. *J. Geophysical Research: Oceans* 112, 1–7. doi: 10.1029/2007JC004095

Matsuoka, K., Skoglund, A., and & Roth, G. (2018) (Quantarctica).

Mawji, E., Gledhill, M., Milton, J. A., Zubkov, M. V., Thompson, A., Wolff, G. A., et al. (2011). Production of siderophore type chelates in Atlantic ocean waters enriched with different carbon and nitrogen sources. *Mar. Chem.* 124, 90–99. doi: 10.1016/j.marchem.2010.12.005

McMahon, C., Hindell, M., Dorr, T., and Massom, R. A. (2002). Winter distribution and abundance of crabeater seals off George V land, East Antarctica. *Antarctic Sci.* 14, 128–133. doi: 10.1017/S0954102002000688

Meier, W. N., Fetterer, F., Windnagel, A. K., and Stewart, S. (2021). "NOAA/NSIDC climate data record of passive microwave Sea ice concentration," in *NSIDC, 4th ed* (Colorado, USA: Boulder).

Morel, F. M., Kustka, A., and Shaked, Y. (2008). The role of unchelated fe in the iron nutrition of phytoplankton. *Limnology Oceanogr.* 53, 400–404. doi: 10.4319/lo.2008.53.1.0400

Nolting, R. F., Gerringa, L. J. A., Swagerman, M. J. W., Timmermans, K. R., and de Baar, H. J. W. (1998). Fe (III) speciation in the high nutrient, low chlorophyll pacific region of the southern ocean. *Mar. Chem.* 62, 335–352. doi: 10.1016/S0304-4203(98)00046-2

Omanović, D., Garnier, C., and Pižeta, I. (2015). ProMCC: An all-in-one tool for trace metal complexation studies. *Mar. Chem.* 173, 25–39. doi: 10.1016/j.marchem.2014.10.011

Orsi, A. H., Whitworth, T., and Nowlin, W. D. (1995). On the meridional extent and fronts of the Antarctic circumpolar current. *Deep Sea Res. Part I: Oceanogr. Res. Papers* 42, 641–673. doi: 10.1016/0967-0637(95)00021-W

Orsi, A., and Wiederwohl, C. (2009). A recount of Ross Sea water. *Deep Sea Res. Part II: Topical Stud. Oceanogr.* 56, 778–795. doi: 10.1016/j.dsr2.2008.10.033

Petschick, R., Kuhn, G., and Gingele, F. (1996). Clay mineral distribution in surface sediments of the south Atlantic: sources, transport, and relation to oceanography. *Mar. Geology* 130, 203–229. doi: 10.1016/0025-3227(95)00148-4

Pižeta, I., Sander, S. G., Hudson, R. J. M., Omanović, D., Baars, O., Barbeau, K. A., et al. (2015). Interpretation of complexometric titration data: An intercomparison of methods for estimating models of trace metal complexation by natural organic ligands. *Mar. Chem.* 173, 3–24. doi: 10.1016/j.marchem.2015.03.006

Poorvin, L., Sander, S. G., Velasquez, I., Ibisanmi, E., LeCleir, G. R., and Wilhelm, S. W. (2011). A comparison of fe bioavailability and binding of a catecholate siderophore with virus-mediated lysates from the marine bacterium vibrio alginolyticus PWH3a. *J. Exp. Mar. Biol. Ecol.* 399, 43–47. doi: 10.1016/j.jembe.2011.01.016

Raiswell, R., Hawkings, J., Elsenousy, A., Death, R., Tranter, M., and Wadham, J. (2018). Iron in glacial systems: Speciation, reactivity, freezing behavior, and alteration during transport. *Front. Earth Sci.* 6. doi: 10.3389/feart.2018.00222

Rivaro, P., Ardini, F., Grotti, M., Aulicino, G., Cotroneo, Y., Fusco, G., et al. (2019). Mesoscale variability related to iron speciation in a coastal Ross Sea area (Antarctica) during summer 2014. *Chem. Ecol.* 35, 1–19. doi: 10.1080/02757540.2018.1531987

Rivaro, P., Ardini, F., Grotti, M., Vivado, D., Salis, A., and Damonte, G. (2021). Detection of carbohydrates in sea ice extracellular polymeric substances *via* solid-phase extraction and HPLC-ESI-MS/MS. *Mar. Chem.* 228, 103911. doi: 10.1016/j.marchem.2020.103911

Ropert-Coudert, Y., Kato, A., Shiomi, K., Barbraud, C., Angelier, F., Delord, K., et al. (2018). Two recent massive breeding failures in an adélie penguin colony call for the creation of a marine protected area in D'Urville Sea/Mertz. *Front. Mar. Sci.* 5. doi: 10.3389/fmars.2018.00264

Rue, E. L., and Bruland, K. W. (1997). The role of organic complexation on ambient iron chemistry in the equatorial pacific ocean and the response of a

mesoscale iron addition experiment. *Limnology Oceanogr.* 42, 901–910. doi: 10.4319/lo.1997.42.5.0901

Sambrotto, R. N., Matsuda, A., Vaillancourt, R., Brown, M., Langdon, C., Jacobs, S. S., et al. (2003). Summer plankton production and nutrient consumption patterns in the mertz glacier region of East Antarctica. *Deep Sea Res. Part II: Topical Stud. Oceanogr.* 50, 1393–1414. doi: 10.1016/S0967-0645(03)00076-6

Sander, S. G., Tian, F., Ibisanmi, E. B., Currie, K. I., Hunter, K. A., and Frew, R. D. (2015). Spatial and seasonal variations of iron speciation in surface waters of the subantarctic front and the otago continental shelf. *Mar. Chem.* 173, 114–124. doi: 10.1016/j.marchem.2014.09.001

Sanvito, F., and Monticelli, D. (2020). Fast iron speciation in seawater by catalytic competitive ligand equilibration-cathodic stripping voltammetry with tenfold sample size reduction. *Analytica Chimica Acta* 1113, 9–17. doi: 10.1016/j.aca.2020.04.002

Sarthou, G., Bucciarelli, E., Chever, F., Hansard, S. P., González-Dávila, M., Santana-Casiano, J. M., et al. (2011). Labile Fe(II) concentrations in the Atlantic sector of the southern ocean along a transect from the subtropical domain to the weddell Sea gyre. *Biogeosciences* 8, 2461–2479. doi: 10.5194/bg-8-2461-2011

Schine, C. M. S., Alderkamp, A.-C., van Dijken, G., Gerringa, L. J. A., Sergi, S., Laan, P., et al. (2021). Massive southern ocean phytoplankton bloom fed by iron of possible hydrothermal origin. *Nat. Commun.* 12, 1211. doi: 10.1038/s41467-021-21339-5

Schlosser, C., de la Rocha, C. L., Streu, P., and Croot, P. L. (2012). Solubility of iron in the southern ocean. *Limnology Oceanogr.* 57, 684–697. doi: 10.4319/lo.2012.57.3.0684

Sedwick, P. N., DiTullio, G. R., and Mackey, D. J. (2000). Iron and manganese in the Ross Sea, Antarctica: Seasonal iron limitation in Antarctic shelf waters. *J. Geophysical Research: Oceans* 105, 11321–11336. doi: 10.1029/2000jc000256

Shadwick, E. H., Rintoul, S. R., Tilbrook, B., Williams, G. D., Young, N., Fraser, A. D., et al (2013). Glacier tongue calving reduced dense water formation and enhanced carbon uptake. *Geophysical Research Letters* 40, 904–09.

Shaked, Y., and Lis, H. (2012). Disassembling iron availability to phytoplankton. *Front. Microbiol.* 3. doi: 10.3389/fmicb.2012.00123

Silvano, A., Rintoul, S. R., and Herraiz-Borreguero, L. (2016). Ocean-ice shelf interaction in East Antarctica. *Oceanography* 29, 130–143. doi: 10.5670/oceanog.2016.105

Slagter, H. A., Gerringa, L. J. A., and Brussaard, C. P. D. (2016). Phytoplankton virus production negatively affected by iron limitation. *Front. Mar. Sci.* 3. doi: 10.3389/fmars.2016.00156

Smith, D. C., and Azam, F. (1992). A simple, economical method for measuring bacterial protein synthesis rates in seawater using 3H-leucine. *Marine Microbial Food Webs* 6, 107–114.

Smith, A. J. R., Ratnarajah, L., Holmes, T. M., Wuttig, K., Townsend, A. T., Westwood, K., et al. (2021). Circumpolar deep water and shelf sediments support late summer microbial iron remineralization. *Global Biogeochem. Cycles* 35, e2020GB006921. doi: 10.1029/2020GB006921

Sutak, R., Camadro, J.-M., and Lesuisse, E. (2020). Iron uptake mechanisms in marine phytoplankton. *Front. Microbiol.* 11. doi: 10.3389/fmicb.2020.566691

Tagliabue, A., Bowie, A. R., DeVries, T., Ellwood, M. J., Landing, W. M., Milne, A., et al. (2019). The interplay between regeneration and scavenging fluxes drives ocean iron cycling. *Nat. Commun.* 10, 4960. doi: 10.1038/s41467-019-12775-5

Tagliabue, A., Sallée, J.-B., Bowie, A. R., Lévy, M., Swart, S., and Boyd, P. W. (2014). Surface-water iron supplies in the southern ocean sustained by deep winter mixing. *Nat. Geosci.* 7, 314. doi: 10.1038/ngeo2101

Tamura, T., Williams, G. D., Fraser, A. D., and Ohshima, K. I. (2012). Potential regime shift in decreased sea ice production after the mertz glacier calving. *Nat. Commun.* 3, 826. doi: 10.1038/ncomms1820

Tani, H., Nishioka, J., Kuma, K., Takata, H., Yamashita, Y., Tanoue, E., et al. (2003). Iron(III) hydroxide solubility and humic-type fluorescent organic matter in the deep water column of the Okhotsk Sea and the northwestern north pacific ocean. *Deep Sea Res. Part I: Oceanogr. Res. Papers* 50, 1063–1078. doi: 10.1016/S0967-0637(03)00098-0

Thuróczy, C.-E., Alderkamp, A.-C., Laan, P., Gerringa, L. J. A., Mills, M. M., Van Dijken, G. L., et al. (2012). Key role of organic complexation of iron in sustaining phytoplankton blooms in the pine island and amundsen polynyas (Southern ocean). *Deep Sea Res. Part II: Topical Stud. Oceanogr.* 71-76, 49–60. doi: 10.1016/j.dsr2.2012.03.009

Thuróczy, C. E., Gerringa, L. J. A., Klunder, M. B., Laan, P., and de Baar, H. J. W. (2011). Observation of consistent trends in the organic complexation of dissolved iron in the Atlantic sector of the southern ocean. *Deep Sea Res. Part II: Topical Stud. Oceanogr.* 58, 2695–2706. doi: 10.1016/j.dsr2.2011.01.002

Tian, F., Frew, R. D., Sander, S., Hunter, K. A., and Ellwood, M. J. (2006). Organic iron(III) speciation in surface transects across a frontal zone: the chatham rise, new Zealand. *Mar. Freshw. Res.* 57, 533–544. doi: 10.1071/MF05209

Tison, J. L., Worby, A., Delille, B., Brabant, F., Papadimitriou, S., Thomas, D., et al. (2008). Temporal evolution of decaying summer first-year sea ice in the Western weddell Sea, Antarctica. *Deep Sea Res. Part II: Topical Stud. Oceanogr.* 55, 975–987. doi: 10.1016/j.dsr2.2007.12.021

Toner, B. M., Santelli, C. M., Marcus, M. A., Wirth, R., Chan, C. S., Mccollom, T., et al. (2009). Biogenic iron oxyhydroxide formation at mid-ocean ridge hydrothermal vents: Juan de fuca ridge. *Geochimica Cosmochimica. Acta* 73, 388–403. doi: 10.1016/j.gca.2008.09.035

Tonnard, M. (2018). *Biogeochemical cycle of iron: distribution and speciation in the north Atlantic ocean (GA01) and the southern ocean (GIpr05) (GEOTRACES)* (Brest, France: University of Tasmania (Australia) and Doctoral School of Marine and Coastal Sciences (Plouzané).

Vaillancourt, R. D., Sambrotto, R. N., Green, S., and Matsuda, A. (2003). Phytoplankton biomass and photosynthetic competency in the summertime mertz glacier region of East Antarctica. *Deep Sea Res. Part II: Topical Stud. Oceanogr.* 50, 1415–1440. doi: 10.1016/S0967-0645(03)00077-8

van der Zee, C., Roberts, D. R., Rancourt, D. G., and Slomp, C. P. (2003). Nanogoethite is the dominant reactive oxyhydroxide phase in lake and marine sediments. *Geology* 31, 993–996. doi: 10.1130/G19924.1

Velasquez, I. B., Ibisanmi, E., Maas, E. W., Boyd, P. W., Nodder, S., and Sander, S. G. (2016). Ferrioxamine siderophores detected amongst iron binding ligands produced during the remineralization of marine particles. *Front. Mar. Sci.* 3. doi: 10.3389/fmars.2016.00172

Waite, T. D., and Morel, F. M. (1984). Photoreductive dissolution of colloidal iron oxides in natural waters. *Environ. Sci. Technol.* 18, 860–868. doi: 10.1021/es00129a010

Westwood, K. J., Thomson, P. G., van den Enden, R. L., Maher, L. E., Wright, S. W., and Davidson, A. T. (2018). Ocean acidification impacts primary and bacterial production in Antarctic coastal waters during austral summer. *J. Exp. Mar. Biol. Ecol.* 498, 46–60. doi: 10.1016/j.jembe.2017.11.003

Whitby, H., Planquette, H., Cassar, N., Bucciarelli, E., Osburn, C. L., Janssen, D. J., et al. (2020). A call for refining the role of humic-like substances in the oceanic iron cycle. *Sci. Rep.* 10, 6144. doi: 10.1038/s41598-020-62266-7

Williams, G. D., Aoki, S., Jacobs, S. S., Rintoul, S. R., Tamura, T., and Bindoff, N. L. (2010). Antarctic Bottom water from the adélie and George V land coast, East Antarctica (140–149°E). *J. Geophysical Research: Oceans* 115, 1–29. doi: 10.1029/2009jc005812

Williams, G. D., Bindoff, N. L., Marsland, S. J., and Rintoul, S. R. (2008). Formation and export of dense shelf water from the adélie depression, East Antarctica. *J. Geophysical Research: Oceans* 113, 1–12. doi: 10.1029/2007JC004346

Wu, J., Boyle, E., Sunda, W., and Wen, L.-S. (2001). Soluble and colloidal iron in the oligotrophic north Atlantic and north pacific. *Science* 293, 847–849. doi: 10.1126/science.1059251

Wuttig, K., Townsend, A. T., van der Merwe, P., Gault-Ringold, M., Holmes, T., Schallenberg, C., et al. (2019). Critical evaluation of a seaFAST system for the analysis of trace metals in marine samples. *Talanta* 197, 653–668. doi: 10.1016/j.talanta.2019.01.047